Nanoparticles Reinforcement for the Improved Strength and High-Temperature Wear Resistance of Mn-Cr Steel

A. Kračun, D. Jenko, M. Godec, S. V. Savilov, G. Prieto, W. Tuckart & B. Podgornik

Metallurgical and Materials Transactions A

ISSN 1073-5623

Metall and Mat Trans A
DOI 10.1007/s11661-018-4833-7

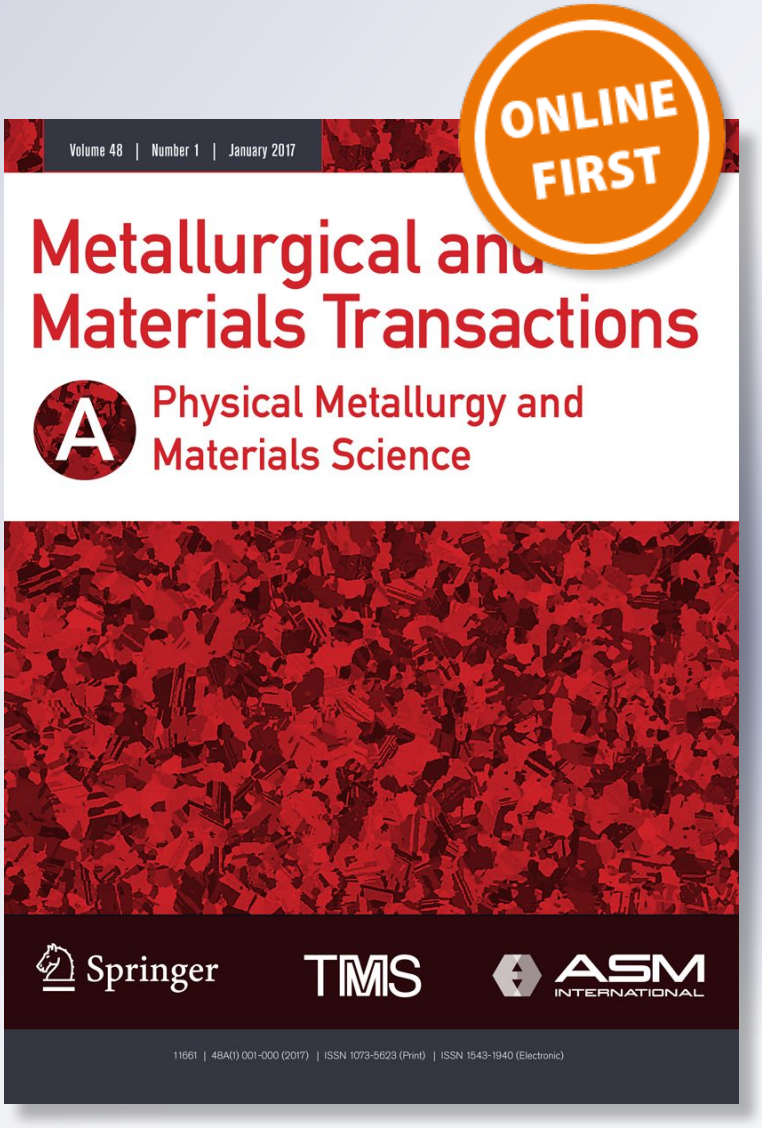

Springer

Nanoparticles Reinforcement for the Improved Strength and High-Temperature Wear Resistance of Mn-Cr Steel

A. KRAČUN, D. JENKO, M. GODEC, S.V. SAVILOV, G. PRIETO, W. TUCKART, and B. PODGORNIK

Nanotechnologies offer tremendous potential when it comes to modifying the microstructure of steel through the incorporation of nanoparticles. While typical production methods for metal-matrix composites are difficult and expensive, conventional casting routes suffer from inhomogeneity and agglomeration of the added nanoparticles. The aim of this study was to investigate the feasibility and possibilities of introducing nanosized particles into a steel matrix through a conventional casting process and to determine the effect of different nanoparticles and methods of incorporation on the strength, toughness, and high-temperature wear resistance of martensitic steel. The results show that also in the case of a conventional casting process, it is possible to obtain a homogeneous distribution of nanoparticles in the metal matrix, resulting in improved strength, maintained toughness, and up to five times better high-temperature wear resistance of the Mn-Cr steel. However, the rate of improvement greatly depends on the method and type of nanoparticles incorporation. The most promising results were observed for the combination of carbon nanotubes, oxide nanoparticles, and dispersant, sealed in a steel tube, with the dispersant providing the uniform distribution, the carbon nanotubes delivering the good toughness and the adhesive wear properties, and the oxide nanoparticles ensuring oxidation and abrasive wear resistance.

https://doi.org/10.1007/s11661-018-4833-7

I. INTRODUCTION

IN recent decades, considerable efforts have been made to develop high- and ultra-high-performance steels,[1,2] mainly to meet the needs for weight and cost savings in the automotive and transportation industries.[3] This is partly due to need for more compact designs and increased safety and partly due to environmental concerns. The environmental aspect is related to reduced CO_2 emissions and improved fuel consumption.[4] In this respect, using lighter components and reducing vehicle weight is one of the key elements. However, lighter components require high-strength materials where an improvement in the strength should not degrade other properties, such as formability, fatigue, and wear resistance.[5] Moreover, maintaining high toughness and fatigue resistance is essential to comply with reliability and safety regulations.[6]

In the case of structural components, the emphasis in material research is focused on increasing the strength and the wear resistance of martensitic steels while maintaining good ductility, toughness, and fatigue properties.[5,7,8] To a certain extent, this can be achieved by controlling the alloy composition, effective heat treatments, micro-alloying, and thermo-mechanical treatments, with the improvement in strength being obtained through grain refinement and the precipitation of fine stable carbides, nitrides, or carbo-nitrides.[9–11] Nanosized precipitates of micro-alloying elements can refine the austenite grain size during heat treatment as well as strengthen the matrix, where the final material properties depend on the size, shape, stability, and distribution uniformity of the particles.[11] However, these traditional techniques offer only a limited rate of improvement, with an increase in one property often being accompanied by a reduction in another.[12]

As a response, different methods of incorporating ceramic particles to reinforce metal matrices and produce composite materials with superior properties have been the subject of intense investigation. The first efforts

A. KRAČUN, D. JENKO, M. GODEC, and B. PODGORNIK are with the Institute of Metals and Technology, Lepi pot 11, 1000 Ljubljana, Slovenia. Contact e-mail: bojan.podgornik@imt.si S.V. SAVILOV is with the M.V. Lomonosov Moscow State University, Leninskie gory 1-3, Moscow, Russia, 119991. G. PRIETO and W. TUCKART are with the Universidad Nacional del Sur, Av. Alem 1253, 8000 Bahía Blanca, Argentina.

Manuscript submitted January 21, 2018.

Published online: 18 July 2018

were directed towards the development of high-performance composites with very high strength and moduli for use in specialized aerospace applications.[13] These were soon followed by the development of low-cost aluminum and steel-matrix composites with inexpensive ceramic particles, which are of commercial interest to different industries.[14–17] Ceramic particulate-reinforced metal-matrix composites (MMCs) combine certain properties of the ceramic reinforcements and the metallic matrix, resulting in attractive physical and mechanical properties, *e.g.*, a high-specific modulus, strength, hardness, thermal stability, and wear resistance.[18] In general, the metal matrix is expected to provide the high ductility and the toughness of the MMCs, while the ceramic reinforcements embedded in the metallic matrix are responsible for the high strength, elastic modulus, wear resistance, high melting point, and low density. Different oxides, carbides, borides, as well as nitrides and carbon nanotubes are incorporated into metals and alloys matrices to produce MMCs with superior physical, mechanical, and wear properties.[19] As such, MMCs have emerged as an important class of high-performance structural materials for use in aerospace, automotive, chemical, and transportation applications requiring superior strength, stiffness, and wear resistance.[20] MMCs can also be tailored to suit the needs of many different applications.[21]

For most of the particle-reinforced MMCs, the typical size of the reinforcing ceramic particles is from several to tens of microns, normally resulting in a considerable reduction in ductility and toughness.[22,23] This is mainly due to the easy initiation and propagation of cracks in the ceramic particles or at the interface. In order to enhance the mechanical properties, the particle size needs to be reduced below the micrometer range.[24] Different investigations indicate that the ductility and toughness of MMCs can be significantly improved with a simultaneous increase in the strength by reducing the particles to the nanometer range, *i.e.*, the so-called nanosized particle-reinforced MMCs.[25,26] However, the main challenge for nanosized MMCs is how to fabricate them. At present, there are two main processing challenges: (1) uniformly dispersing the nanosized particles in the metal matrix and (2) achieving a strong interfacial bond.[24]

Over the past 30 years, different processing routes, such as powder metallurgy, spray deposition, mechanical alloying and infiltration, ultrasonic cavitational-based solidification, and high-temperature self-propagating synthesis have been developed.[27] These methods typically require expensive and sophisticated equipment, have high manufacturing costs, low productivity, and can suffer from the thermodynamic instability of the reinforcement in the metal matrix at the region of the interface,[14,28] and are thus not suitable for the large-scale production of structural components. On the other hand, the casting routes employing liquid steel metallurgy are considered to be the most suitable for bulk production. The advantages of casting routes lie in their simplicity, flexibility, and applicability to large-quantity production and are thus the most economical for the production of MMCs and allow very large components to be fabricated.[29] Another advantage of these methods over powder metallurgy is that a cleaner and stronger interface between the particles and the matrix can be achieved, contributing to improved performance.[27]

In general, the solidification synthesis of MMCs involves producing a melt of the selected matrix material followed by the introduction of reinforcement particles into the melt in order to obtain a suitable dispersion.[29] The next step is the solidification of the melt under selected conditions to obtain the desired distribution of the dispersed phase in the cast matrix. When preparing MMCs using the casting methods, there are several factors that need a lot of attention, especially when it comes to nanosized reinforcement particles. These include the difficulty in achieving a uniform distribution of the reinforcement material, the wettability between the two main substances, the porosity in the cast MMCs, and the chemical reactions between the reinforcement particles and the matrix alloy. A homogeneous dispersion of ceramic nanoparticles in molten metals is extremely hard to achieve.[30] Because of the low wettability and the large surface area of the nanosized particles, they tend to agglomerate into coarse clusters along the grain boundaries, not to be homogeneously dispersed throughout the matrix, and the optimal exploitation of the strengthening potential is lost. A homogeneous dispersion becomes even more difficult when the specific weight of the molten metal increases, making it difficult to apply to steels. Thus, liquid metal casting processes are mainly restricted to lightweight MMCs.[30] Consequently, only limited studies exist that report the successful incorporation of nanosized particles into steel using conventional casting routes.[6,30–32]

The aim of the present study was to investigate the feasibility and possibilities of introducing nanosized particles into a steel matrix through a conventional low-cost liquid metal casting process and to determine the effect of different reinforcement nanoparticles and the method of incorporation on the strength, toughness, and high-temperature wear resistance of Mn-Cr martensitic steel.

II. EXPERIMENTAL

A. *Material Processing*

The material used in this investigation as a reference and starting base material was commercial Mn-Cr alloyed martensitic steel (AISI 6150(H)) with a carbon content of about 0.5 pct, 1.0 pct Mn, and 1.0 pct Cr, used for springs, highly stressed automotive forgings, and components subjected to fatigue and wear. The steel melt was produced under normal atmospheric conditions using a 20 kg capacity medium-frequency induction furnace. After melting the starting material and adding the required ferroalloys to cover the melting losses, different types of reinforcing nanoparticles were introduced into the melt in concentrations between 0.05 and 2.5 pct.

The first group, aimed at investigating the effect of the nanoparticle type, included three different types of nanoparticles (TiO_2, Al_2O_3 and multi-walled carbon nanotubes—CNTs), added to molten steel in a 0.1 pct concentration. The TiO_2 and Al_2O_3 nanoparticles were commercially available nanoparticles (US-Nano) with a purity of > 99.9 pct and an average size of 30 to 50 nm. Multi-walled CNTs with diameters of 10 to 30 nm were synthesized by the catalytic pyrolysis of hexane over an MgO support promoted by Co-Mo nanoparticles.[33] The catalytic support was obtained using common techniques by the thermal decomposition of a mixture of $Mg(NO_3)_2{\cdot}6H_2O$, $Co(NO_3)_2{\cdot}6H_2O$, $(NH_4)_2Mo_2O_7$, citric acid, and glycine at 750 °C under a N_2 flow. The CNT synthesis was conducted at the same temperature with the introduction of hexane to a quartz tubular reactor using N_2. The obtained material was annealed in air for 4 hours at 400 °C to remove the amorphous carbon impurities and then washed with a HCl solution for 3 hours and then with water at neutral pH.[34] A total of 10 g of particular nanoparticles were mixed with Fe powder in a 1:15 ratio and sintered into a cylinder, which was immersed into the melt, held in the melt for 90 seconds, and then the melt was poured into the mold.

The second set of experiments was focused on the method of *ex situ* introduction of the reinforcement nanoparticles into the melt. Besides the nanoparticles being mixed with Fe powder, sintered into a cylinder, and immersed into the melt, three additional techniques were used in this investigation. These included nanoparticles being sealed in a thin steel tube and poured over with molten metal, nanoparticles being sealed in a 100 × 100 × 100 mm^3 steel cube and inserted into the melt, or nanoparticles being simply placed at the bottom of the mold and poured over with molten metal. In this case, TiO_2 and Al_2O_3 nanoparticles with a size of 30 to 50 nm and a 0.1 pct concentration were used.

In the case of MMCs, the biggest obstacle is the agglomeration and non-uniform distribution of the reinforcement particles in the metal matrix, which is greatly dependent on the particle size and concentration.[27,35] Therefore, the next group of experiments was aimed at investigating the effect of the reinforcement particles' size and concentration. For this reason, Al_2O_3 particles of two different sizes (50 and 500 nm) and four different concentrations (0.05, 0.1, 0.5, and 2.5 pct) were introduced using the sealed-tube technique.

The final set of experiments was focused on a study of the combined effect of carbon nanotubes and oxide nanoparticles. It was expected that stabilization of the particles at the CNT surface due to molecular-level mixing would prevent their aggregation. Again, nano-sized particles/carbon nanotubes were added in a 0.1 pct concentration using the sealed-cube technique. However, in this case, the carbon nanotubes were further processed in order to obtain a $CNTs/Al_2O_3$ composite. The procedure involved the dispersion of CNTs in an aqua solution of $Al(NO_3)_3{\cdot}9H_2O$ in an ultrasonic bath

Table I. Experimental Conditions and Nanoparticles Reinforced Mn-Cr Steel Charges Prepared in this Investigation

Spec.	Base Material	Nanoparticles		Particles Size (nm)	Particles Concent.	Method	Dispersant	
Nanoparticle type								
R	6150(H)	—		—	—	—	—	
T	6150(H)	TiO_2		30 to 50	0.1 pct	sintered cylinder	—	
A	6150(H)	Al_2O_3		30 to 50	0.1 pct	sintered cylinder	—	
C	6150(H)	CNTs		10 to 30	0.1 pct	sintered cylinder	—	
Method of introduction								
OS	6150(H)	Al_2O_3/TiO_2		30 to 50	0.1 pct	sintered cylinder	—	
OC	6150(H)	Al_2O_3/TiO_2		30 to 50	0.1 pct	sealed in steel cube	—	
OT	6150(H)	Al_2O_3/TiO_2		30 to 50	0.1 pct	sealed in steel tube	—	
OP	6150(H)	Al_2O_3/TiO_2		30 to 50	0.1 pct	powder	—	
Nanoparticles concentration and size								
A50	304	Al_2O_3		30 to 50	0.1, 0.5, 1.0, 2.5	sealed in steel tube	—	
A500	304	Al_2O_3		500	0.1, 0.5, 1.0, 2.5	sealed in steel tube	—	
A500 + D	304	Al_2O_3		500	2.5	sealed in steel tube	CaSi	1:1
Combination of CNTs and Al_2O_3								
C + D	6150(H)	CNTs		10 to 30	0.1	sealed in steel cube	Methylene	10 pct
C/A	6150(H)	$CNTs/Al_2O_3$	1:1	10 to 50	0.1	sealed in steel cube	—	
C/A + D	6150(H)	$CNTs/Al_2O_3$	1:1	10 to 50	0.1	sealed in steel cube	Methylene	10 pct
C/4A + D	6150(H)	$CNTs/Al_2O_3$	1:4	10 to 50	0.15	sealed in steel cube	Methylene	10 pct

R, reference material; T, TiO_2 nanoparticles, sintered Fe cylinder; A, Al_2O_3 nanoparticles, sintered Fe cylinder; C, carbon nanotubes, sintered Fe cylinder; OS, oxide nanoparticles, sintered Fe cylinder; OC, oxide nanoparticles, sealed in steel cube; OT, oxide nanoparticles, sealed in steel tube; OP, oxide nanoparticles, used as a powder; A50, Al_2O_3 nanoparticles, size 30 to 50 nm; A500, Al_2O_3 nanoparticles, size 500 nm; A500 + D, Al_2O_3 nanoparticles, size 500 nm, added dispersant; C + D, carbon nanotubes, added dispersant; C/A, carbon nanotubes + Al_2O_3 nanoparticles; C/A + D, carbon nanotubes + Al_2O_3 nanoparticles (1:1), added dispersant; C/4A + D, carbon nanotubes + Al_2O_3 nanoparticles (1:4), added dispersant.

for 8 hours or by ultrasonication using a Vibra Cell VCX-750 generator for 4 hours in order to reach CNTs/Al_2O_3 ratios of 1:4 and 1:1, respectively. Subsequently, ammonia solution was slowly added to the resulting suspension with vigorous stirring until a basic pH was reached. The obtained gel was filtered and washed with distilled water, dried at 130 °C for 12 hours, and finally annealed at 430 °C for 3 hours. Furthermore, the carbon nanotubes/Al_2O_3 nanoparticles composite powder was additionally mixed with a dispersion agent (*i.e.*, CaSi, Metylan glue, *etc.*) in a 1:1 ratio, in order to facilitate a more uniform and homogeneous distribution of reinforcing nanoparticles in the metal matrix. A detailed list of all the experimental conditions and setups used in this investigation is given in Table I.

After casting, the ingots were hot rolled from 1150 °C in five passes, achieving an overall deformation rate of 2.5 and a final thickness of 20 mm, and then air cooled. Test specimens were then machined from the middle of the ingot, being oriented in the rolling direction and then given a vacuum heat treatment and a final surface polishing (R_a = 0.05 μm). The vacuum heat treatment was performed in a vacuum furnace with uniform high-pressure gas-quenching using nitrogen gas at a pressure of 5 bar ($\lambda_{800\text{-}500}$ = 0.42), an austenitizing temperature of 880 °C (soaking time 10 minutes), and a single 1 hour tempering at 375 °C. The vacuum heat treatment resulted in an average hardness of about 52 HRc, with the difference between different experimental ingots being within the measurement uncertainty (±1 HRc).

B. *Characterization*

The nanoparticle-reinforced steel specimens were first characterized in terms of microstructural analysis, including identification of the reinforcing nanoparticles and their distribution uniformity, the volume fraction of the incorporated nanoparticles, changes caused within the metal matrix, and the type of interface. Microstructural analyses were performed using a JEOL JSM6500F scanning electron microscope, a JEOL JEM 2100F high-resolution transmission electron microscope (HR-TEM), and VG-Scientific MICROLAB 310F high-resolution field-emission Auger microprobe (HRAES).

C. *Strength and Toughness Properties*

The effect of the nanoparticles' addition and the method of introduction on the strength and toughness of the Mn-Cr steel included tensile tests and measurements of the impact and fracture toughness. The tensile tests at room temperature (21 °C ± 0.5 °C) according to the ISO 6892-1 standard were performed on standard cylindrical specimens with a diameter of 10 mm and a gauge length of 50 mm using Instron 8802 tensile-test machine. The measurements performed on three parallel samples involved a determination of the yield strength $R_{p0.2}$, the ultimate tensile strength R_m, and the elongation A_5.

The impact toughness was determined according to the Charpy V-notch test (BS EN 10045-1) using a 300-J pendulum. Testing was carried out at room temperature (21 °C ± 0.5 °C) on three consecutive specimens and the average impact toughness was calculated. On the other hand, for the fracture-toughness measurements, non-standard, circumferentially notched and pre-cracked tension bar (CNPTB) specimens were used (Figure 1), with the fatigue pre-crack of about 0.5 mm created under rotating-bending loading (600 N, 4500 cycles).[36] By subjecting the CNPTB specimen to tensile loading and measuring the load at fracture and the diameter of brittle fractured area, the fracture toughness was calculated according to the procedure described in Reference 37. In order to obtain statistically relevant results, up to eight CNPTB specimens were prepared and tested for each experimental setup.

D. *Tribological Testing*

Tribological testing of the nanoparticle-reinforced Mn-Cr steel was performed under unidirectional sliding conditions using a block-on-ring configuration (Figure 2). Tests where the Mn-Cr steel block (~ 15 × 10 × 6.5 mm^3) was loaded against a hardened AISI 1045 carbon steel ring (ϕ36 mm; ~ 54 HRc) were performed at a load of 20 N (p_H = 100 MPa) and a sliding speed of 0.03 m/s. Due to the fact that high-temperature wear applications are becoming increasingly important, the tests were performed at three different temperatures, 20 °C, 150 °C, and 300 °C, with three repetitions for each condition and each test specimen. The testing time

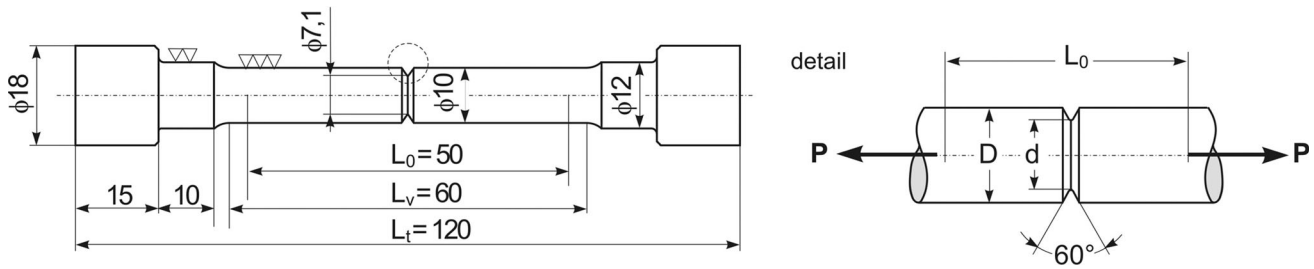

Fig. 1—Schematic of the CNPTB test specimen; all dimensions given in mm. Reprinted with permission from Ref. [36] copyright ASTM international, 100 Barr Harbor Drive, West Conshohocken, PA 19428.

was 26 minutes, corresponding to an overall sliding distance of 50 m. During testing, the coefficient of friction was monitored continuously and the wear of the Mn-Cr block was analyzed with optical profilometry (Alicona Infinite Focus G4) after the test. During the wear measurements, the abrasive and adhesive wear components were determined, with the volume of the material being removed from the contact surface identified as the abrasive wear and the volume of the carbon steel disc adhered to the contact surface of the test block being the adhesive wear (Figure 3).

III. RESULTS AND DISCUSSION

A. *Type of Nanoparticles*

The vacuum-heat-treated reference Mn-Cr steel shows the microstructure of tempered martensite with a number of small secondary carbides uniformly distributed in the matrix (Figure 4(a)). The TEM analysis revealed cementite lamellas with a thickness of about 15 nm and a spacing of ~ 70 nm (Figure 5(a)).

The martensitic microstructure of the reference Mn-Cr steel, obtained by quenching it from 880 °C and single tempering at 375 °C, resulted in a high yield strength (YS) of ~ 1650 MPa, an ultimate tensile strength (UTS) of 1720 MPa, and an elongation at fracture in the range of 10 pct, as shown in Figure 6. On the other hand, the reference Mn-Cr steel shows relatively poor toughness properties, with a fracture toughness of 25 MPa$\sqrt{m}$ and an impact toughness of ~ 6 J (Figure 7). Introducing the oxide nanoparticles led to an increased strength of the Mn-Cr steel. In the case of the TiO_2 nanoparticles, the strength increased by 5 to 10 pct, resulting in a UTS of over 1900 MPa, while maintaining the toughness properties. Furthermore, the introduction of TiO_2 nanoparticles even improved the elastic properties of the Mn-Cr steel, increasing the elongation at fracture to ~ 12 pct. Al_2O_3 nanoparticles, on the other hand, also gave improved strength to the Mn-Cr steel ($R_m \approx 1900$ MPa), but hampered its toughness and elastic properties, showing a reduction of about 10 pct (Figures 6 and 7).

Also in the case of oxide nanoparticles, the microstructure of the Mn-Cr steel consists of tempered martensite with unchanged spacing and thickness for the cementite lamellas. However, besides the uniformly distributed fine secondary carbides, some small circular particles of approx. 50 nm in size can also be observed (Figure 4(b)), providing increased strength. In the case of the Al_2O_3 nanoparticles, these inclusions were confirmed to be Al oxides. Furthermore, the AES line-scan analysis (Figure 8) indicates the successful incorporation of Al_2O_3 nanoparticles in the steel matrix with a clear interface and no signs of intermetallic reactions, thus preventing a considerable drop in the toughness properties. Also for TiO_2 nanoparticles, fine circular inclusions of ~ 50 nm were observed. However, these are not oxides, but different Ti-based precipitates (Figure 5(b)). The thermodynamic simulations suggest that the TiO_2 is not thermodynamically favored when added to the molten steel. It is suggested that the TiO_2 nanoparticles dissolve in the matrix when added to the liquid steel, which produces metallic titanium and oxygen. The Ti then reacts with the surrounding elements like N, C, and S and promotes the formation of Ti-based precipitates, *i.e.*, TiC, Ti(C,N), *etc.*[38] Consequently, an improved strength, while maintaining good toughness properties, can be obtained through the

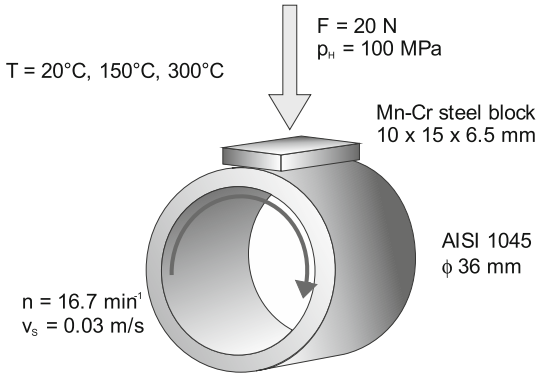

Fig. 2—Tribological test configuration.

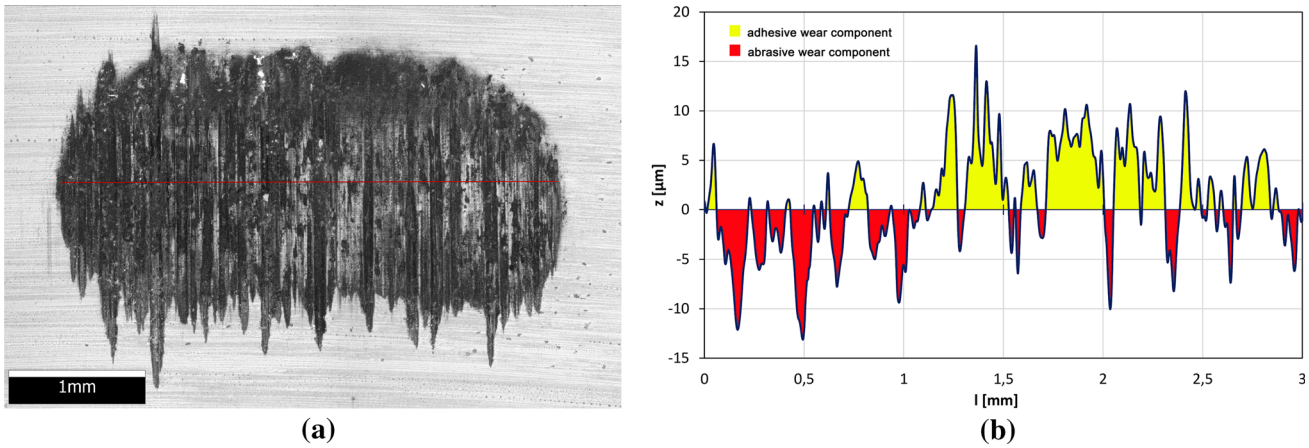

Fig. 3—Identification of the adhesive and abrasive wear components; (*a*) wear scar and (*b*) 2D surface profile.

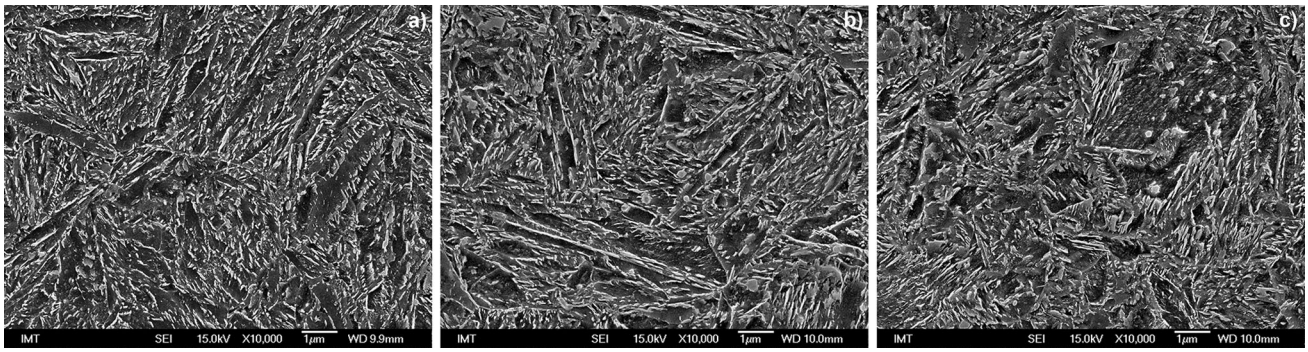

Fig. 4—SEM micrographs of the microstructure for (*a*) reference Mn-Cr steel, (*b*) Mn-Cr steel with added Al_2O_3 nanoparticles, and (c) Mn-Cr steel with added CNTs.

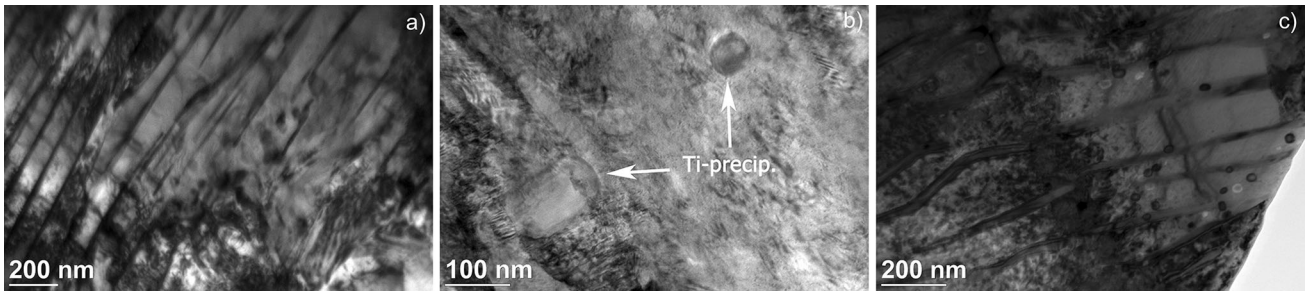

Fig. 5—TEM micrographs for (*a*) reference Mn-Cr steel, (*b*) Mn-Cr steel with added TiO_2 nanoparticles, and (*c*) Mn-Cr steel with added CNTs.

addition of TiO_2 nanoparticles, as shown in Figures 6 and 7.

Finally, for the Mn-Cr steel with added CNTs, the microstructure of tempered martensite equivalent to the reference steel without any clear indications of CNT incorporation was identified. However, the introduction of CNTs led to an increased thickness and spacing of the cementite lamellas, with the thickness being increased from 15 to about 30 nm and the spacing from 70 to over 100 nm, as shown in Figure 5(c). At the same time, the "CNT-alloyed" Mn-Cr steel shows a strength improvement comparable to the TiO_2 nanoparticles, while providing superior toughness, *i.e.*, 10 to 15 pct above the reference Mn-Cr steel, as shown in Figures 6 and 7.

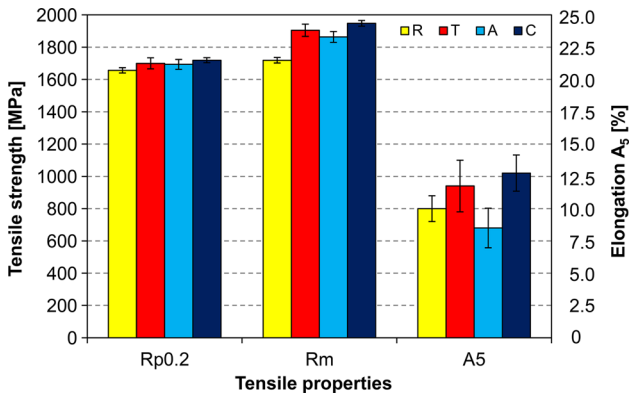

Fig. 6—Effect of nanoparticle type on the tensile properties of Mn-Cr steel.

B. *Method of Incorporation*

As shown by the results in Figure 9, changing from a sintered cylinder (OS) to the oxide nanoparticles being sealed in a steel cube and incorporated into the melt (OC) provided a similar strength for the Mn-Cr steel ($R_m \approx 1900$ MPa), but about 10 pct better toughness ($K_{Ic} \approx 26$ MPa$\sqrt{m}$). A further improvement in tensile strength, with the UTS approaching 2000 MPa, while maintaining a high fracture toughness, was obtained when the oxide nanoparticles were sealed in a thin steel tube and poured over with the melt (OT). However, if the oxide-nanoparticles powder is simply placed in the mold and molten metal poured over it (OP), this can even result in a deterioration of the steel's strength and toughness properties, as shown in Figure 9. The same trends were observed for the TiO_2 and Al_2O_3 nanoparticles.

When sealed in the steel cube and, even more so, the steel tube, the nanoparticles are more gradually exposed and wetted by the molten metal, thus creating more favorable conditions for restrained agglomeration and more homogeneous distribution and incorporation of oxide nanoparticles in the metal matrix. On the other hand, if nanoparticles are used as the powder, it will promote agglomeration and the formation of large, more complex, non-metallic inclusions and clusters (Figure 10) with a negative effect on the steel's properties.[39]

C. *Size and Concentration of Nanoparticles*

The effects of nanoparticle size and concentration on the homogeneity of the distribution and the rate of nanoparticle incorporation into the metal matrix are shown in Figure 11. This time Al_2O_3 nanoparticles and AISI 304 stainless steel with a single-phase microstructure were used as the reinforcing particles and the metal matrix, respectively; this allows easier nanoparticle detection and identification. An analysis was made on twenty randomly acquired digital micrographs to determine the population density of the nanoparticles, measured as the count per 100 μm^2. In the case of the 50-nm particles added in a concentration of 0.1 to 0.5 pct, about one particle per 100 μm^2 was incorporated into the metal matrix, being more or less uniformly distributed throughout the whole volume of the cast ingot (Top, Middle and Bottom). The same is also true for concentrations of up to 1 pct, as shown in Figure 10. However, as the concentration of the added nanoparticles was increased to 2.5 pct, the number of incorporated particles also increased to ~ 1.5 per 100 μm^2 and the distribution became less uniform.

For larger Al_2O_3 nanoparticles (500 nm), the number and uniform distribution of the incorporated particles was the same as for the small ones (~ 1 particle/100 μm^2) until added in concentrations below 0.5 pct. In the case of the larger concentrations of 1 and 2.5 pct, the number of incorporated particles increased to about 1.5 and 3 particles/100 μm^2, respectively. Furthermore, the population density also became non-homogeneous, with the density increased from the bottom towards the top of the cast ingot, as shown in Figure 11. However, if a dispersion agent is added to the nanoparticle powder, facilitating dispersion of the particles within the melt, a uniform distribution can also be obtained for larger particles and higher concentrations (> 1 pct).

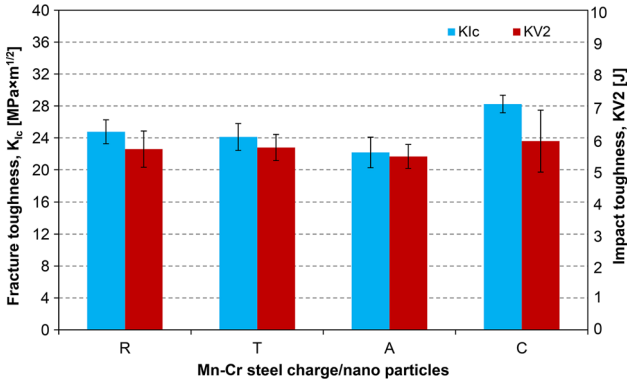

Fig. 7—Effect of nanoparticle type on the toughness properties of Mn-Cr steel.

D. *Combined Effect of CNTs and Al_2O_3 Nanoparticles*

For the investigation of the effect of two filling agents, *i.e.*, CNTs and Al_2O_3, a nanosized CNTs/Al_2O_3 composite where the oxide phase is stabilized at the nanotube surfaces was synthesized using the sol–gel technique. The experimental procedure applied resulted in a uniform distribution of CNTs in the oxide matrix, as shown in Figure 12. According to the size and concentration research results (Section III–C), 10 pct of dispersant (Methylene blue) was also added to the CNTs/Al_2O_3 composite powder and introduced into the melt using the steel-cube technique.

The use of a dispersant and the introduction of nanoparticles using the steel-cube technique further improved the tensile properties of the CNT-reinforced Mn-Cr steel (~ 10 pct), increasing the YS to 1840 MPa,

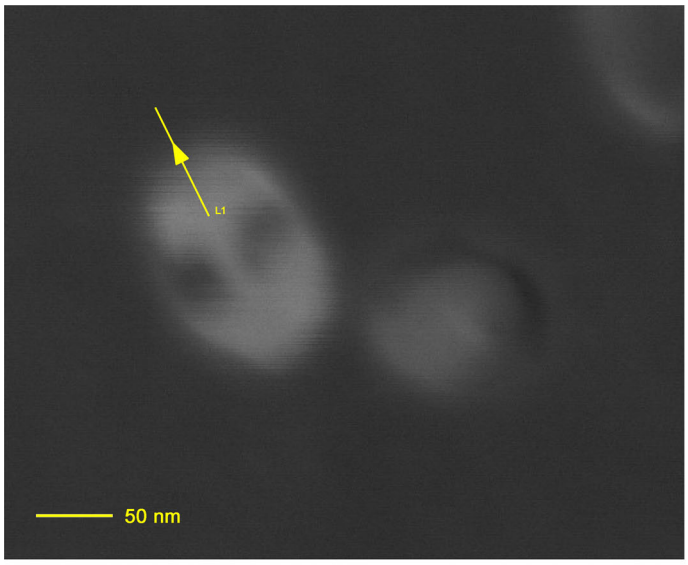

(a)

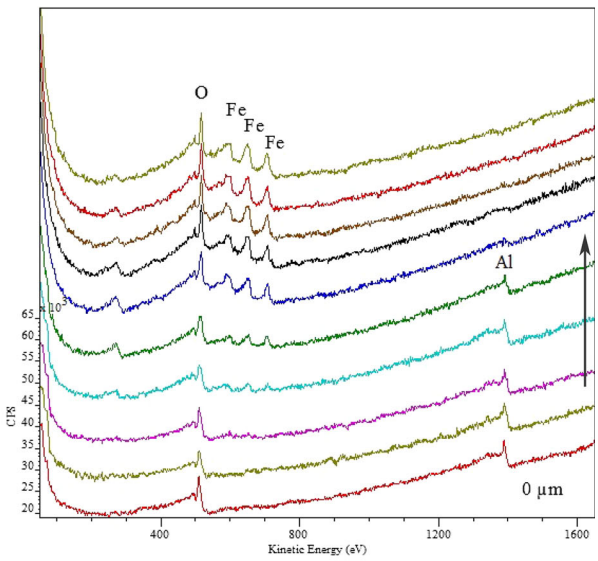

(b)

Fig. 8—AES analysis of Al_2O_3 nanoparticle incorporated in the investigated steel matrix; (*a*) micrograph with arrow indicating line analysis position and direction and (*b*) individual AES spectra along the analyzed line, shown from the bottom to the top.

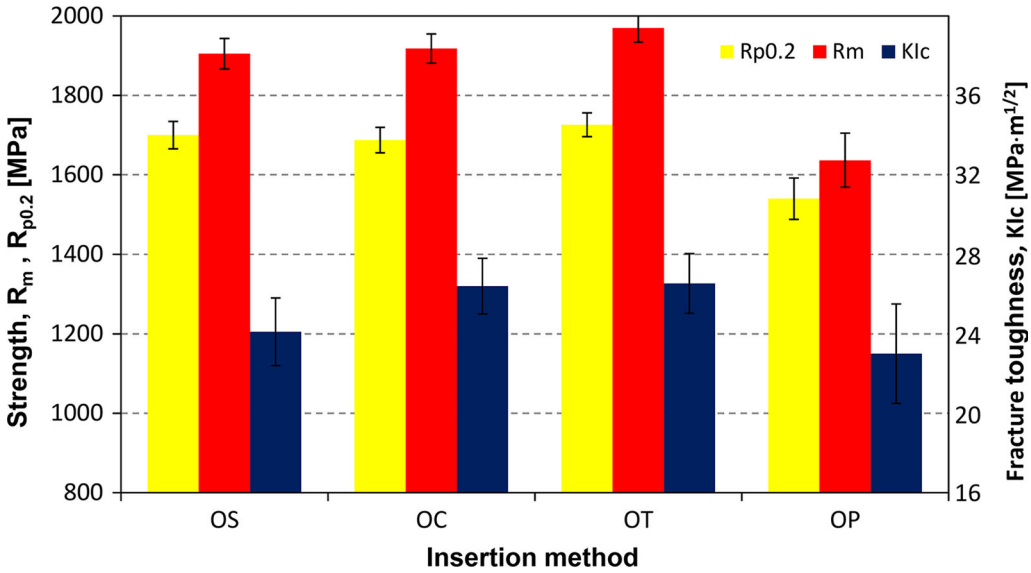

Fig. 9—Effect of the nanoparticle incorporation method on the tensile and toughness properties of the Mn-Cr steel.

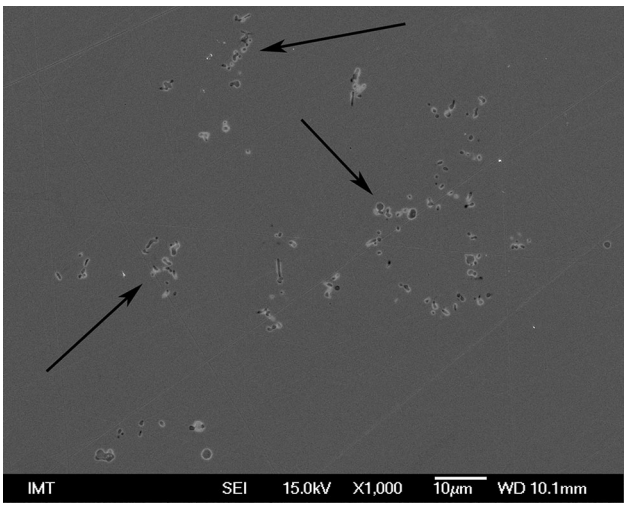

Fig. 10—Al_2O_3 nanoparticles agglomeration and clustering (indicated by arrows) when used as a powder (OP).

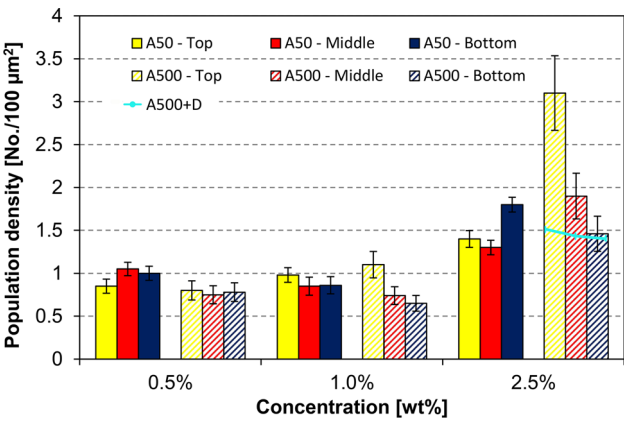

Fig. 11—Effect of Al_2O_3 particles size and concentration on the distribution homogeneity and population density.

the UTS to 2000 MPa, and the impact toughness to about 6.5 J (Figure 13). However, the combination of CNTs and Al_2O_3 nanoparticles (C/A + D) had no positive effect on the tensile and toughness properties of the investigated steel. In contrast, the properties were reduced to the level of Mn-Cr steel reinforced only with oxide particles, *i.e.*, a strength reduction of 3 to 4 pct and toughness by 5 to 10 pct, with the drop in the properties intensifying when increasing the Al_2O_3 content, as shown in Figure 13. However, if the dispersant is also omitted (C/A), which results in a noticeable agglomeration and non-homogeneous distribution of reinforcing particles, a considerable drop in properties, even below the reference steel, can take place.

E. *Tribological Properties*

Finally, the effect of the nanoparticles inclusion on the sliding wear resistance of the Mn-Cr steel was investigated at room and elevated temperatures, and then compared to the reference non-modified Mn-Cr steel. At room temperature, the average coefficient of friction for the Mn-Cr steel sliding against hardened AISI 1045 carbon steel was 0.4, regardless of whether, which, and how these nanoparticles were included in the melt. Steady-state conditions were reached after about 180 seconds or 5 m of sliding. A slightly higher steady-state coefficient of friction of 0.45, reached after 250 seconds or 8 m of sliding, was found for the testing temperature of 150 °C, which was more or less identical for all the specimens tested. In the case of the room temperature and 150 °C testing the worn surface exhibited a combination of abrasive and adhesive wear, as shown in Figure 14. However, as the testing temperature was increased to 300 °C, the surface oxidation and abrasive wear became dominant and a steady-state coefficient of friction was reached after about 100 seconds or 3 m of sliding, depending on the specimen type. The highest coefficient of friction of ~ 0.7 was observed for the

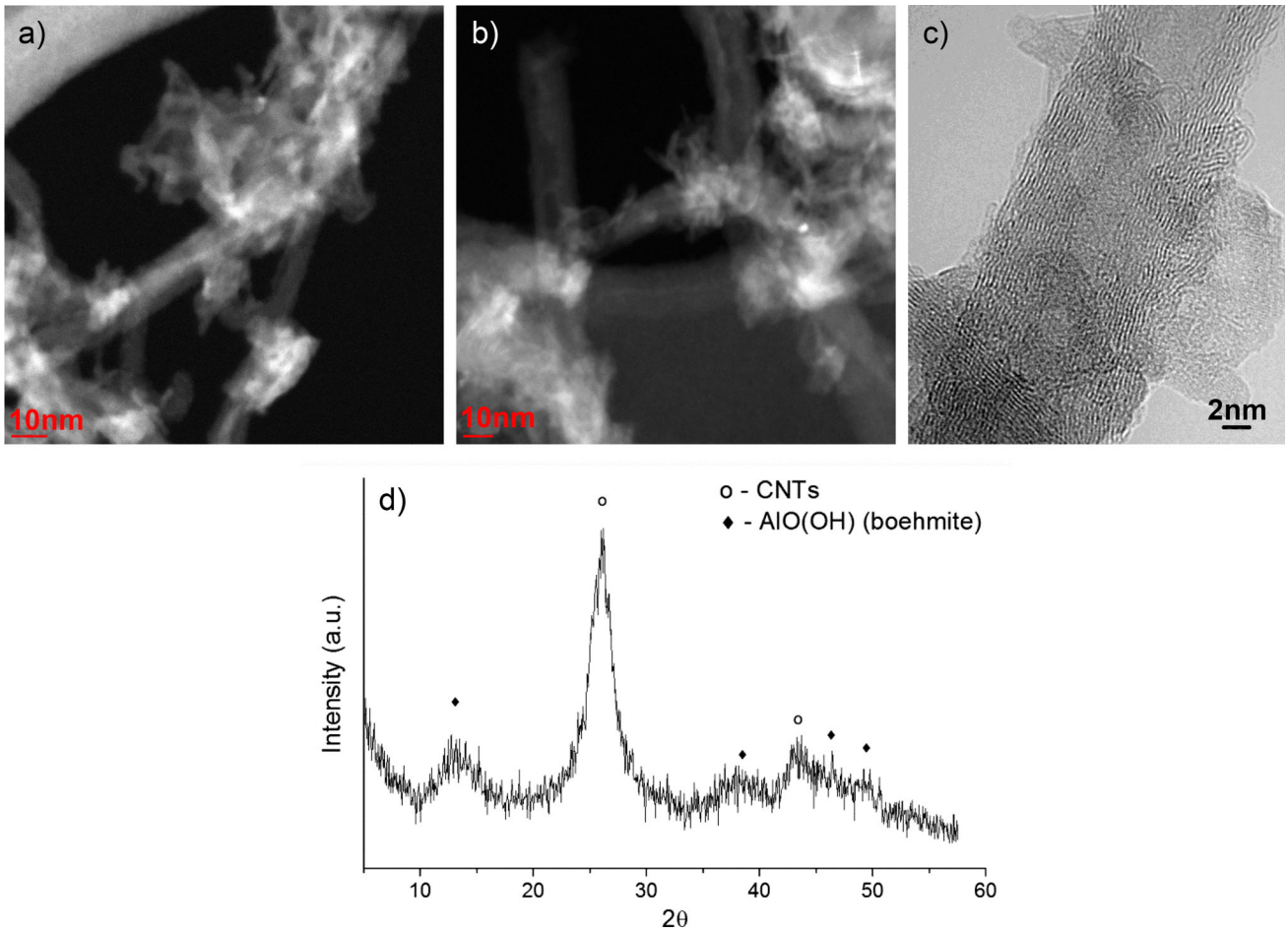

Fig. 12—TEM (*a*) and (*b*), HRTEM (*c*), and XRD spectrum (*d*) from CNTs/Al_2O_3 composite synthesized by sol-gel technique.

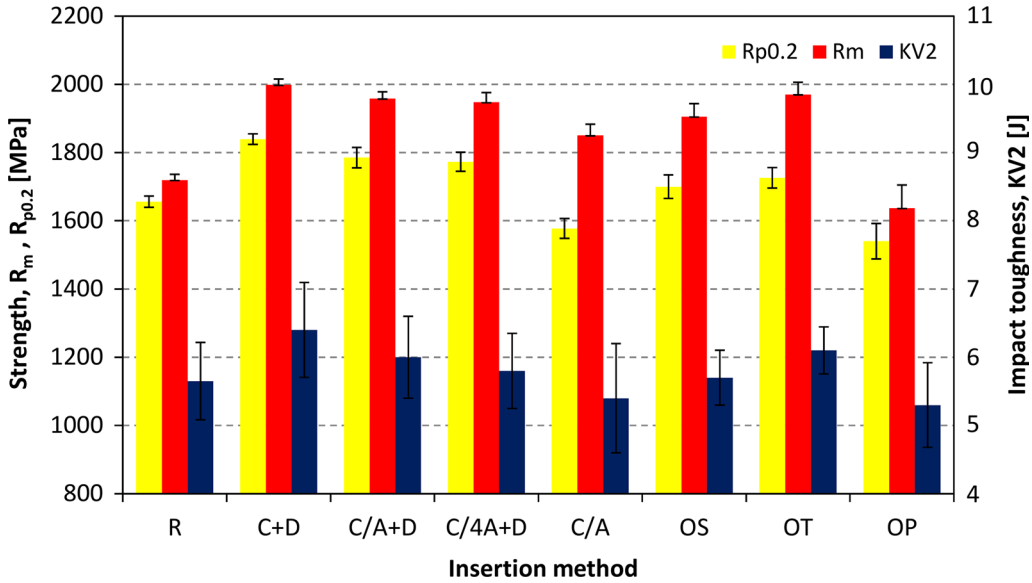

Fig. 13—Effect of CNT/Al_2O_3 composite and dispersant on the strength and impact toughness.

reference, non-modified Mn-Cr steel, 0.65 for Al_2O_3 nanoparticles, 0.6 for CNTs, and 0.55 for TiO_2 nanoparticles.

The results for the wear resistance are shown in Figure 15. In the case of room temperature and the reference Mn-Cr steel, the abrasive (material removed

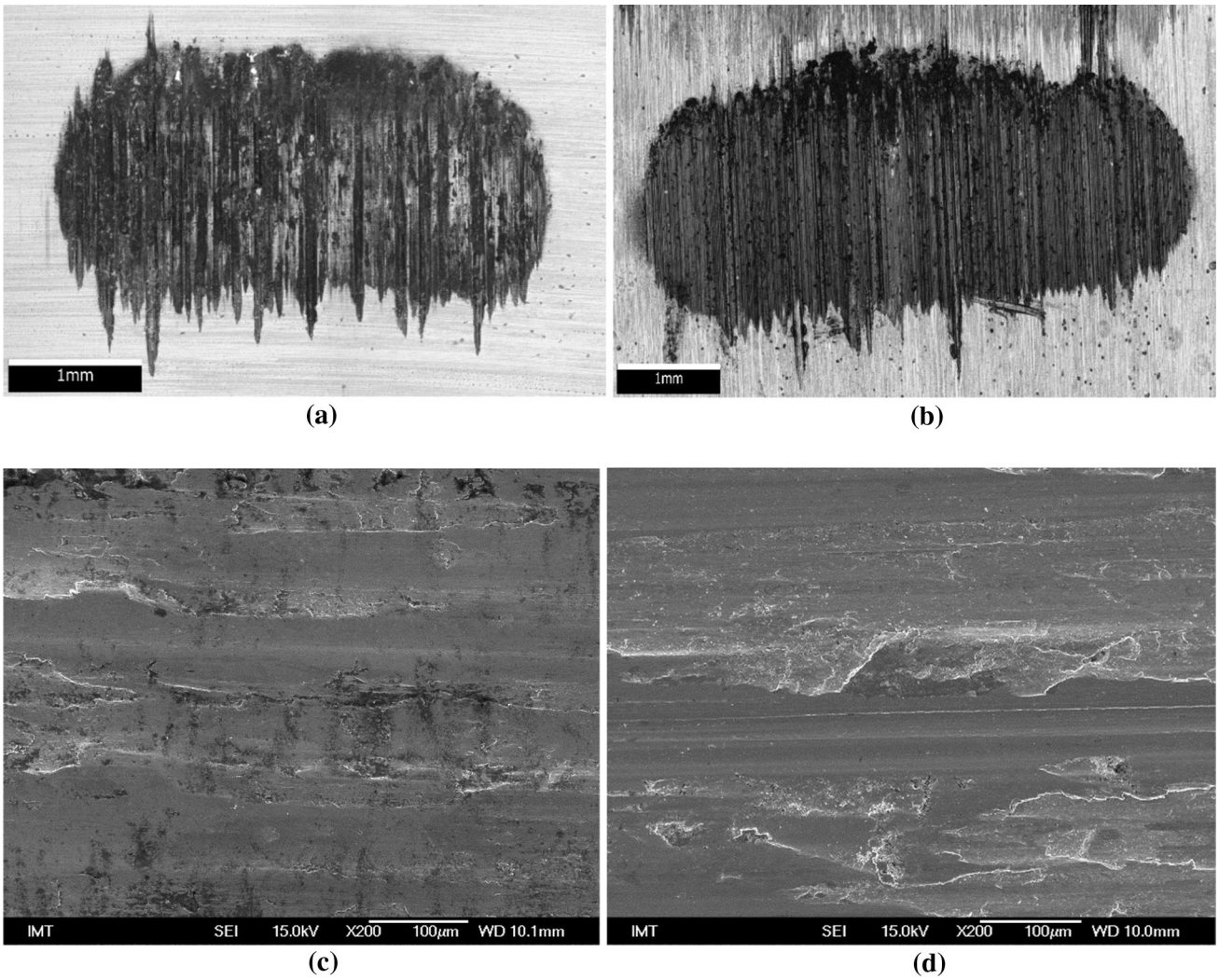

Fig. 14—OM and SEM micrographs of a typical worn surface for reference steel; (*a*) and (*c*) room/moderate temperature and (*b*) and (*d*) 300 °C.

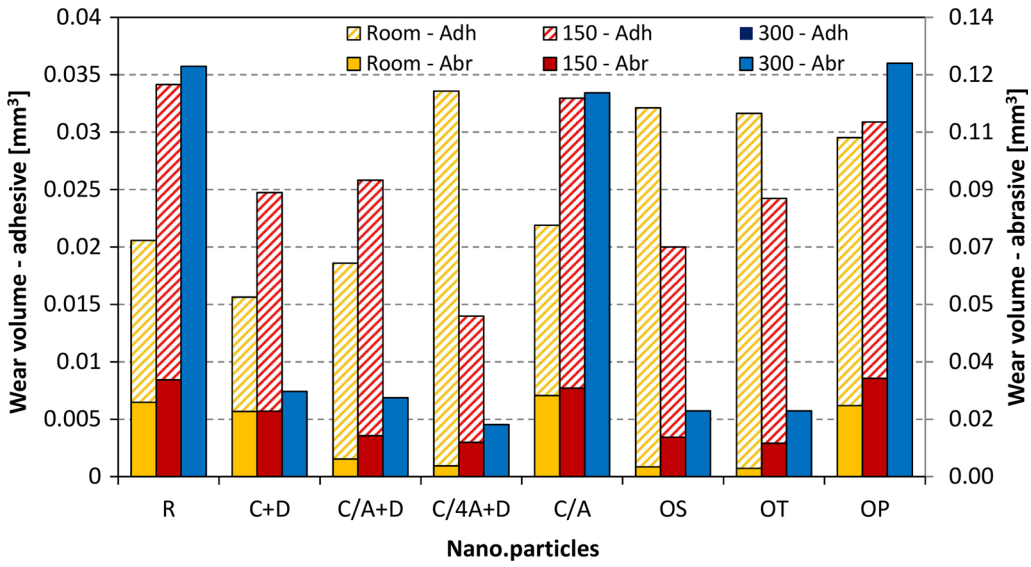

Fig. 15—Wear volume for room- and elevated-temperature testing.

from the surface) and adhesive wear-volume components (material adhered) were of the same size, *i.e.*, ~ 0.02 mm^3. Adding CNTs to the melt reduced the wear volume, especially the adhesive component, reducing it to 0.015 mm^3. On the other hand, if the CNTs were mixed with Al_2O_3 nanoparticles, this substantially improves the abrasive wear resistance, but deteriorates the adhesive component. When used in a 1:1 ratio (CNTs:Al_2O_3), the abrasive wear volume was reduced to 0.005 mm^3 and the adhesive value increased back to 0.02 mm^3. A further increase in the Al_2O_3 content (1:4) gave a further 50 to 60 pct improvement in the abrasive wear resistance, but made the steel more than two times more susceptible to adhesion, as shown in Figure 15.

If oxide nanoparticles are used without dispersant, the agglomeration of particles and the formation of clusters will instead of improving the abrasive wear resistance lead to an increase in both the adhesive and abrasive wear. Also in the case of TiO_2 nanoparticles, although not being directly incorporated into the metal matrix, but rather forming Ti-based nanoprecipitates, a superior abrasive wear resistance is obtained, with the abrasive wear-volume component being reduced down to 0.003 mm^3. However, superior abrasive wear resistance comes at the expense of adhesive wear, which was increased up to as much as 0.032 mm^3. As shown in Figure 15, the method of nanoparticle incorporation has a more-or-less negligible effect on the tribological properties of Mn-Cr steel, as long as a considerable agglomeration of the nanoparticles is prevented, *i.e.*, the use of dispersant and sealing the nanoparticle powder in a tube or cube. Thus, simply placing a nanoparticle powder in the mold and pouring molten steel over it will result in deteriorated tribological properties, with the highest level of adhesive and abrasive wear.

Increasing the testing temperature to 150 °C led to increased wear of the investigated Mn-Cr steel, mainly in terms of adhesive wear, *i.e.*, the abrasive component by ~ 30 pct and the adhesive component by 70 pct, as compared to the room temperature tests (Figure 15). The same trend was also observed for the Mn-Cr steel reinforced with CNTs, but still giving ~ 40 pct better wear resistance than the reference non-modified Mn-Cr steel. However, by adding oxide nanoparticles with high oxidation and temperature stability,[40] better abrasive but mainly adhesive wear resistance was obtained. Superior wear resistance was shown by combining CNTs and a high volume fraction of Al_2O_3 nanoparticles, followed by TiO_2 nanoparticles. Finally, for testing at 300 °C, a pronounced surface oxidation of the Mn-Cr steel took place, leaving abrasive wear as the main wear mechanism, as shown in Figure 14(b). For the reference non-modified Mn-Cr steel, the wear volume increased to ~ 0.12 mm^3. However, the introduction of nanoparticles, especially temperature-resistant oxide nanoparticles, resulted in reduced surface oxidation and an up to 5 times better high-temperature wear resistance.

At room and moderate temperatures, an increased strength combined with a high toughness, provided by the CNTs, mixed with a small amount of nanoparticles, is essential for obtaining a high level of both abrasive and adhesive wear resistance. On the other hand, at high temperatures, the oxidation and temperature stabilities of the oxide nanoparticles become predominant in providing a superior wear resistance for the Mn-Cr steel. However, also in the case of high-temperature tests, a non-uniform distribution and agglomeration of nanoparticles as well as the formation of complex non-metallic inclusions, can, instead of the expected improvement, result in a deterioration of the high-temperature wear resistance, as shown in Figure 15.

IV. CONCLUSION

The results of this investigation can be summarized in the following conclusions:

1. Through the proper incorporation method, nanoparticles can also be successfully introduced into a metal matrix and improve the properties of Mn-Cr steel by using conventional casting routes. In the case of Al_2O_3 nanoparticles, the successful incorporation with a clear interface and no signs of any intermetallic reactions at the nanoparticle/steel-matrix interface is obtained, thus giving the steel an improved strength. However, this is not the case for TiO_2 nanoparticles. Their dissolution leads to the formation of Ti-based nanoprecipitates, resulting in a good combination of high strength and toughness. Also for the carbon nanotubes, there is no clear indication of their direct incorporation into the steel matrix, although there is an increase in the cementite lamellas' thickness and spacing, leading to a superior combination of high strength and toughness.
2. For the methods investigated, the best results were obtained when the nanoparticles are sealed into a thin steel tube and poured over with molten steel. The use of a dispersant retards the particles' agglomeration and further improves their homogeneous distribution, which is also facilitated for larger particles and higher particle concentrations. However, if the nanoparticles are used in too high concentrations or directly in powder form, substantial agglomeration and cluster formation can lead to a deterioration in the properties.
3. In terms of tribological properties, beneficial results are obtained when combining CNTs and oxide nanoparticles. As shown by this investigation, CNTs provide improved adhesive wear resistance and oxide nanoparticles improved the abrasive component. This is especially important in the case of high-temperature high-abrasion applications where up to five times better wear resistance is provided by increasing the content of oxidation- and temperature-resistant oxide nanoparticles. However, under room and moderate temperatures, oxide nanoparticles show a strong tendency for adhesion and therefore low concentrations should be used in situations dominated by adhesion. Furthermore, if the nanoparticles' agglomeration and clustering take place, this will lead to particles

being removed from the contact surface and a consequent deterioration in the wear resistance.

ACKNOWLEDGMENTS

The authors acknowledge the financial support from the Slovenian Research Agency (Research Core Funding Nos. P2-0050 and P2-0231, applied research project L2-7599, as well as BI-AR/15-017-007 and BI-RU/14-15-012 bilateral projects). The authors would also like to acknowledge help from M. Torkar and F. Tehovnik from the Institute of Metals and Technology for the melting and casting, A. Egorov, S. Chernyak, and R. Novotortsev from M.V. Lomonosov Moscow State University for preparing the carbon nanotubes and their composites with Al_2O_3, as well as T. Ahačič, S. Šolič, and M. Pečar from Institute of Metals and Technology for mechanical testing, and SEM and AES analysis.

REFERENCES

1. R. Kuziak, R. Kawalla, and S. Waengler: *Arch. Civ. Mech. Eng.*, 2008, vol. 8, pp. 103–17.
2. G. Jha, S. Das, S. Sinha, A. Lodh, and A. Haldar: *Mater. Sci. Eng. A*, 2013, vol. 561, pp. 394–402.
3. W.J. Nam, C.S. Lee, and D.Y. Ban: *Mater. Sci. Eng. A*, 2000, vol. 289, pp. 8–17.
4. P.K. Mallick: *Materials, Design and Manufacturing for Lightweight Vehicles*, Woodhead Publishing Limited, Cambridge, 2010.
5. F. Ozturk, A. Polat, S. Toros, and R.C. Picu: *J. Iron Steel Res. Int.*, 2013, vol. 20, pp. 68–74.
6. B. Podgornik, M. Torkar, J. Burja, M. Godec, and B. Senčič: *Mater. Sci. Eng. A*, 2015, vol. 638, pp. 183–89.
7. B. Podgornik, V. Leskovšek, M. Godec, and B. Senčič: *Mater. Sci. Eng. A*, 2014, vol. 599, pp. 81–86.
8. B. Nie, Z. Zhang, Z. Zhao, and Q. Zhong: *Mater. Des.*, 2013, vol. 50, pp. 503–08.
9. C. Zhang, Y. Liu, C. Jiang, and J. Xiao: *J. Iron Steel Res. Int.*, 2011, vol. 18, pp. 49–53.
10. C. Zhang, Y. Liu, L. Zhou, and C. Jiang: *J. Iron Steel Res. Int.*, 2012, vol. 19, pp. 47–51.
11. W. Zhou, H. Guo, Z. Xie, X. Wang, and C. Shang: *Mater. Sci. Eng. A*, 2013, vol. 587, pp. 365–71.
12. A.A. Barani, F. Li, P. Romano, D. Ponge, and D. Raabe: *Mater. Sci. Eng. A*, 2007, vol. 463, pp. 138–146.
13. E. Pagounis and V.K. Lindroos: *Mater. Sci. Eng. A*, 1998, vol. 246, pp. 221–34.
14. I.A. Ibrahim, F.A. Mohamed, and E.J. Lavernia: *J. Mater. Sci.*, 1991, vol. 26, pp. 1137–56.
15. D.J. Lloyd: *Int. Mater. Rev.*, 1994, vol. 39, pp. 1–23.
16. A. Luo: *Metall. Mater. Trans. A*, 1995, vol. 26A, pp. 2445–55.
17. K.U. Kainer: *Metal Matrix Composites. Custom-Made Materials for Automotive and Aerospace Engineering*, Wiley, Weinheim, 2003.
18. F. Akhtar: *Can. Metall. Q.*, 2014, vol. 53, pp. 253–63.
19. F. Akhtar, S. Guo, J. Askari, and J. Tian: *J. Univ. Sci. Technol. B*, 2007, vol. 14, pp. 89–93.
20. S.C. Tjong and K.C. Lau: *Mater. Lett.*, 1999, vol. 41, pp. 153–58.
21. I. Sulima, P. Klimczyk, and P. Malczewski: *Acta Metall. Sin.*, 2014, vol. 27, pp. 12–18.
22. X.W. Zeng, W.G. Zhang, N. Wei, R.P. Liu, and M.Z. Ma: *Mater. Sci. Eng. A*, 2007, vol. 443, pp. 224–28.
23. Q.C. Jiang, X.L. Li, and H.Y. Wang: *Scripta Mater.*, 2003, vol. 48, pp. 713–17.
24. Dongshuai. Zhou, Feng. Qiu, Huiyuan. Wang, and Qichuan. Jiang: *Acta Metall. Sin.*, 2014, vol. 27, pp. 798–805.
25. M. Bahrami, K. Dehghani, and M.K.B. Givi: *Mater. Des.*, 2014, vol. 53, pp. 217–25.
26. D.S. Zhou, F. Qiu, and Q.C. Jiang: *Mater. Sci. Eng. A*, 2014, vol. 596, pp. 98–102.
27. S. Chen, P. Seda, M. Krugla, and A. Rijkenberg: *Mater. Sci. Tech.*, 2016, vol. 32, pp. 992–1003.
28. K.I. Parashivamurthy, M.N. Chandrasekharaiah, P. Sampathkumaran, and S. Seetharamu: *Mater. Manuf. Process.*, 2006, vol. 21, pp. 473–78.
29. J. Hashim, L. Looney, and M.S.J. Hashmi: *J. Mater. Process. Tech.*, 1999, vols. 92–93, pp. 1–7.
30. J.-J. Park, S.-M. Hong, E.-K. Park, K.-Y. Kim, M.-K. Lee, and C.-K. Rhee: *Mater. Sci. Eng. A*, 2014, vol. 613, pp. 217–23.
31. S.-H. Lee, S.-M. Hong, B.-S. Han, J.-J. Park, J.-K. Lee, J.-G. Lee, M.-K. Lee, and C.-K. Rhee: *J. Nanosci. Nanotechno.*, 2010, vol. 10, pp. 258–62.
32. R. Lazarova, R.H. Petrov, V. Gaydarova, A. Davidkov, A. Alexeev, M. Manchev, and V. Manolov: *Mater. Design.*, 2011, vol. 32, pp. 2734–41.
33. S.A. Chernyak, A.S. Ivanov, N.E. Strokova, K.I. Maslakov, S.V. Savilov, and V.V. Lunin: *J. Phys. Chem. C*, 2016, vol. 120, pp. 17465–74.
34. S.A. Chernyak, E.V. Suslova, A.S. Ivanov, A.V. Egorov, K.I. Maslakov, S.V. Savilov, and V.V. Lunin: *Appl. Catal. A*, 2016, vol. 523, pp. 221–29.
35. F. Velasco, W.M. Lima, N. Anton, J. Abenojar, and J.M. Torralba: *Tribol. Int.*, 2003, vol. 36, pp. 547–51.
36. B. Podgornik, B. Zuzek, and V. Leskovsek: *Mater. Perform. Charact.*, 2014, vol. 3, pp. 87–103.
37. E.E. Gdoutos: *Fracture Mechanics Criteria and Applications*, Kluwer Academic Publishers, London, 1990.
38. Z. Amondarain, M. Arribas, J.L. Arana, and G.A. Lopez: *Mater. Trans.*, 2013, vol. 54, pp. 1867–76.
39. B. Podgornik and V. Leskovšek: *Metall. Mater. Trans. A*, 2013, vol. 44A, pp. 5694–5702.
40. M. Fernández-Garcia and J.A. Rodriguez: in *Encyclopedia of Inorganic Chemistry,* Wiley, 2009. https://doi.org/10.1002/0470862106.ia377.